Severe acute respiratory syndrome coronavirus spike protein expressed by attenuated vaccinia virus protectively immunizes mice

Himani Bisht*, Anjeanette Roberts†, Leatrice Vogel†, Alexander Bukreyev†, Peter L. Collins†, Brian R. Murphy†, Kanta Subbarao†, and Bernard Moss*‡

*Laboratory of Viral Diseases and †Laboratory of Infectious Diseases, National Institute of Allergy and Infectious Diseases, National Institutes of Health, Bethesda, MD 20892

Contributed by Bernard Moss, March 19, 2004

The spike protein (S), a membrane component of severe acute respiratory syndrome coronavirus (SARS-CoV) is anticipated to be an important component of candidate vaccines. We constructed recombinant forms of the highly attenuated modified vaccinia virus Ankara (MVA) containing the gene encoding full-length SARS-CoV S with and without a C-terminal epitope tag called MVA/S-HA and MVA/S, respectively. Cells infected with MVA/S or MVA/S-HA synthesized a 200-kDa protein, which was recognized by antibody raised against a synthetic peptide of SARS-CoV S or the epitope tag in Western blot analyses. Further studies indicated that S was N-glycosylated and migrated in SDS polyacrylamide gels with an apparent mass of ≈160 kDa after treatment with peptide N-glycosidase F. The acquisition of resistance to endoglycosidase H indicated trafficking of S to the medial Golgi compartment, and confocal microscopy showed that S was transported to the cell surface. Intranasal or intramuscular inoculations of BALB/c mice with MVA/S produced serum antibodies that recognized the SARS S in ELISA and neutralized SARS-CoV *in vitro*. Moreover, MVA/S administered by either route elicited protective immunity, as shown by reduced titers of SARS-CoV in the upper and lower respiratory tracts of mice after challenge. Passive transfer of serum from mice immunized with MVA/S to naïve mice also reduced the replication of SARS-CoV in the respiratory tract after challenge, demonstrating a role for antibody to S in protection. The attenuated nature of MVA and the ability of MVA/S to induce neutralizing antibody that protects mice support further development of this candidate vaccine.

Severe acute respiratory syndrome (SARS), an emerging infectious disease of humans, appeared in China in November 2002 and spread to 30 countries in early 2003. Before the epidemic ended, 8,098 probable cases of SARS and 774 associated deaths were reported to the World Health Organization (www.cdc.gov/mmwr/mguide_sars.html). The etiologic agent of SARS was identified as a coronavirus (CoV) (1–4) and the genome sequence established it as a new member of the family (5, 6). Closely related CoVs were recovered from civet cats and other animals in southern China, although the source of human SARS infections is uncertain (7). Other members of the CoV family can cause fatal diseases of livestock, poultry, and laboratory rodents (8). The two previously identified human CoVs, however, cause only mild upper respiratory infections (8).

All CoVs encode a common set of structural components that include a nucleocapsid protein and three integral membrane proteins, namely the transmembrane protein, the envelope protein, and the spike protein (S) (9, 10). The latter is a type-I transmembrane glycoprotein, which forms the characteristic corona of large protruding spikes on the virion surface and mediates binding to the host cell receptor and membrane fusion. In previously studied CoVs, S was shown to be an important determinant of pathogenesis as well as the major target of protective immunity (8, 11). The SARS-CoV S is quite divergent from those of other CoVs, exhibiting only 20–27% overall amino acid identity (5). Recent studies indicated that the SARS-CoV S is expressed as a noncleaved glycoprotein with an apparent mass of 180–200 kDa that interacts with a functional receptor identified as angiotensin-converting enzyme 2 (12, 13).

Although the 2002/2003 epidemic was eventually controlled by case isolation, the high morbidity and mortality, lack of specific treatment, and potential of reemergence make it imperative to develop effective means to prevent or cure the disease should it reappear. As an initial step, a rodent animal model was developed in which SARS-CoV replicates but does not cause disease (14). Importantly, prior infection or transfer of convalescent serum prevented replication of SARS-CoV in the respiratory tract of mice. The purpose of the present study was to determine whether expression of the S alone could raise neutralizing antibodies and protectively immunize mice.

Vaccinia virus vectors, including the highly attenuated modified vaccinia virus Ankara (MVA) strain, have been used to express and characterize glycoproteins of numerous pathogens, and some of those are being evaluated as candidate prophylactic and therapeutic vaccines (15). MVA accumulated multiple deletions and other mutations during >500 passages in chicken embryo fibroblasts (CEFs) (16–18), resulting in a severe host range restriction in most mammalian cells (19–21). Because the restriction occurs at a late stage of virus assembly, MVA expresses viral and recombinant proteins in nonpermissive as well as in permissive cells (22). MVA is highly attenuated due to its replication defect in mammalian cells, and no adverse effects were reported even when high doses of MVA were given to immune deficient nonhuman primates (23) or severe combined immunodeficiency disease mice (24). Here, we show that the full-length S of SARS-CoV, expressed by MVA, induces binding and neutralizing antibody and protectively immunizes mice against a subsequent infection with SARS-CoV.

Materials and Methods

Viruses and Cells. Primary CEF cells prepared from 10-day-old embryos were grown in minimum essential medium supplemented with 10% FBS and was used to propagate and titer MVA and recombinant MVA strains.

Recombinant Virus Construction. The 3,768-nt ORF encoding the SARS-CoV S of the Urbani strain was copied and amplified from SARS-CoV virion RNA by RT-PCR, and was cloned and sequenced. A clone was identified that exactly matched the published sequence (GenBank accession no. AY278741). Two poxvirus transcription termination motifs (TTTTTNT) in S were altered by using the QuikChange multisite-directed mu-

Abbreviations: SARS, severe acute respiratory syndrome; CoV, coronavirus; S, spike protein; CEF, chicken embryo fibroblast; MVA, modified vaccinia virus Ankara; pfu, plaque forming unit; HA, hemagglutinin; endo, endoglycosidase; PNGase, peptide N-glycosidase; i.n. intranasally; $TCID_{50}$, tissue culture 50% infective dose.

‡To whom correspondence should be addressed. E-mail: bmoss@niaid.nih.gov.

MEDICAL SCIENCES

tagenesis kit (Invitrogen). After mutagenesis, the entire S gene was PCR-amplified with or without an influenza virus hemagglutinin (HA) epitope tag and inserted into the *Xma*I site of the pLW44 transfer vector (provided by L. Wyatt, National Institutes of Health), bringing it under the control of the vaccinia virus modified H5 early late promoter (25) and adjacent to the gene encoding enhanced GFP regulated by the vaccinia virus P11 late promoter. The correct sequence of the entire S DNA insert was confirmed and recombinant MVAs were made by transfecting transfer plasmids into CEF that were infected with 0.05 plaque forming units (pfu) of MVA per cell. Florescent plaques were cloned by six successive rounds of plaque isolation, propagated in CEF, and purified by sedimentation through a sucrose cushion (26). Titers of MVA/S and MVA/S-HA were determined by staining plaques with anti-vaccinia virus rabbit and anti-HA mouse antibodies, respectively.

Western Blotting. CEF and HeLa cells were infected with 5 pfu of recombinant MVA for 18 h. Infected cells were lysed in ice-cold RIPA buffer [50 mM Tris·HCl (pH 7.5)/150 mM NaCl/1% Triton X-100/0.1% SDS/0.5% sodium deoxycholate] supplemented with protease inhibitor mixture (Sigma). Lysates were kept on ice for 10 min, were centrifuged, and were resolved by SDS/PAGE on a Bistris [bis(2-hydroxyethyl)amino]tris(hydroxymethyl)methane 4–12% polyacrylamide gel. Proteins were transferred to a nitrocellulose membrane, blocked with 5% skimmed milk in PBS, and incubated for 1 h at room temperature with anti-HA mouse mAb (Covance Research Products, Berkeley, CA) or anti-SARS-CoV S rabbit polyclonal antibody (IMG-541, Imgenex, San Diego) diluted 1:1,000 or 1:500 in blocking buffer, respectively. The membrane was washed in PBS containing Tween-20 (0.1%) and was incubated for 1 h with horseradish peroxidase-conjugated anti-mouse and anti-rabbit secondary antibody (Calbiochem) diluted 1:2,000. The membrane was washed and proteins were visualized with the Super Signal chemiluminescence substrate (Pierce).

Endoglycosidase (endo) H and Peptide N-Glycosidase (PNGase) F Treatments. Cleared cell lysates were incubated with 20 μl of anti-HA affinity matrix (Roche Applied Science, Indianapolis) overnight at 4°C. The agarose beads were washed and incubated with endo H and PNGase F (New England Biolabs) according to manufacturer's instructions, and the proteins were analyzed by Western blotting using peroxidase-conjugated anti-HA mouse mAb (Roche Applied Science).

Pulse–Chase Analysis. HeLa cells were mock-infected or infected with 5 pfu per cell of MVA or MVA/S-HA, and 18 h later were incubated for 30 min in DMEM lacking methionine and cysteine, labeled with 100 μCi (1 Ci = 37 GBq) of [^{35}S]methionine and [^{35}S]cysteine per ml of medium for 10 min, washed and chased with medium supplemented with 2 mM methionine and 2 mM cysteine. At each time, cells were harvested, lysed in ice-cold RIPA buffer, and clarified lysates were incubated with 20 μl of anti-HA affinity matrix overnight at 4°C as above. Washed agarose beads were treated with endo H and the samples were resolved by SDS/PAGE and detected by autoradiography.

Confocal Microscopy. CEF or HeLa cells on coverslips were infected with 5 pfu per cell of MVA, MVA/S, or MVA/S-HA, incubated for 18 h, and were either left unfixed and unpermeabilized or fixed with cold 4% paraformaldehyde in PBS for 20 min at room temperature and permeabilized with 2.5% digitonin in PBS for 5 min on ice. The coverslips were washed and incubated with anti-SARS mouse serum kindly provided by L. Anderson (Centers for Disease Control, Atlanta) or anti-HA mouse mAb for 1 h at room temperature, were washed again, and were incubated with Alexa 594-conjugated-anti-mouse IgG (Molecular Probes) diluted in PBS containing 10% FBS for 30 min at room temperature. Coverslips were mounted in 20% glycerol and examined with an inverted confocal microscope.

ELISA. A 96-well plate was coated overnight at 4°C with 50 ng per well of soluble recombinant protein containing the S1 domain of SARS-CoV S made in insect cells, blocked with 5% skimmed milk in PBS containing 0.2% Tween-20 for 1 h at 37°C, and incubated with two-fold dilutions of serum from unimmunized or immunized mice for 1 h at 37°C. After extensive washes, the plate was incubated for 1 h with horse radish peroxidase-conjugated secondary anti-mouse antibody (Roche Applied Science) diluted in blocking buffer, washed again and incubated with substrate solution (3,3′-5,5′-tetramethylbenzidine, Roche Applied Science). The difference in absorbance at 370 and 492 nm was determined, readings from wells lacking antigen were subtracted, and endpoint titers were calculated when the absorbance difference was <0.1.

Neutralization Assay. Neutralizing antibody was determined by the inhibition of cytopathic effects mediated by SARS-CoV on Vero cell monolayers as described (14). The dilution of serum that completely prevented cytopathic effect in 50% of the wells was calculated (27).

Animal Challenge Experiments. Groups of eight BALB/c mice were inoculated intranasally (i.n.) or i.m. with 10^7 pfu of MVA or MVA/S at 0 and 4 weeks. Four weeks after the second immunization, animals were challenged i.n. with 10^4 tissue culture 50% infective dose ($TCID_{50}$) of SARS-CoV as described (14). Two days later, the lungs and nasal turbinates of four animals in each group were removed and the SARS-CoV titers were determined (14).

To obtain serum for passive protection studies, two groups of eight BALB/c mice received MVA/S or MVA i.m. at 0 and 4 weeks. Three weeks after the last immunization, sera were collected and pooled. Undiluted or diluted MVA/S or MVA serum in a total volume of 0.4 ml was injected i.p. in two to four naïve mice. Mice were bled the following day to determine their levels of SARS-CoV-specific neutralizing antibody, and then each was challenged with 10^5 $TCID_{50}$ of SARS-CoV and analyzed as above.

Results

Characterization of SARS-CoV S Expressed by Recombinant MVA. A cDNA clone containing the entire ORF encoding SARS-CoV S was modified by introducing silent mutations that eliminated two poxvirus transcription termination signals and was placed under the control of a vaccinia virus early/late promoter (mH5) and inserted by homologous recombination into the site of an existing deletion (del III) within the MVA genome to produce MVA/S (Fig. 1*A*). We also constructed a second recombinant virus, MVA/S-HA, with a 9-aa HA epitope tag coding sequence at the end of the S ORF. In each case, the gene encoding GFP regulated by a vaccinia virus promoter was coinserted into the MVA genome to facilitate the screening and isolation of recombinant viruses by repeated plaque purifications. Both viruses replicated well in CEF, and the SARS-CoV S insert was genetically stable, as assayed by plaque immunostaining with S-specific antibodies.

A protein doublet with an estimated mass of ≈200 kDa, significantly higher than the value of 135 kDa for the unmodified protein predicted from the nucleotide sequence, was detected by SDS/PAGE of lysates of cells infected with MVA/S and MVA/S-HA and Western blotting with polyclonal antibody to S or a mAb to HA (Fig. 1*B* and data for MVA/S not shown). In addition, some S was trapped near the top of the gel, presumably due to aggregates or oligomers that were not dissociated by treatment with SDS and reducing agent at 100°C.

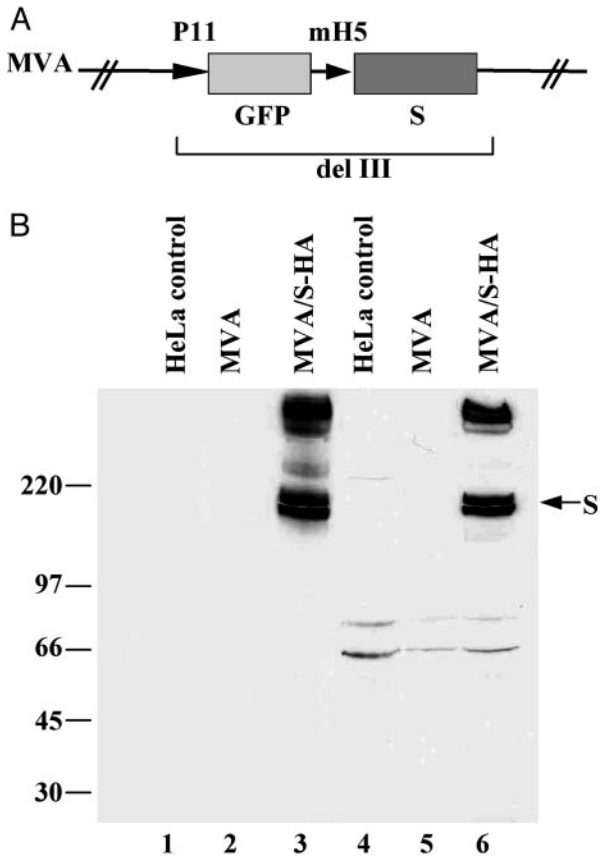

Fig. 1. Expression of SARS-CoV S by recombinant MVA. (*A*) Diagram of selected portion of MVA/S. The GFP and S ORFs were inserted into a deletion site (del III) of the MVA genome. The early/late mH5 and late P11 vaccinia virus promoters regulate S and GFP, respectively. MVA/S-HA has an identical structure except for the presence of a short segment of DNA encoding the influenza virus HA tag at the C terminus of S. (*B*) Western blot analysis of SARS-CoV S protein. HeLa cells were uninfected (control) or infected with MVA or MVA/S-HA. After 18 h, the cells were harvested, the cleared cell lysates were analyzed by SDS/PAGE, and the proteins were transferred to a nitrocellulose membrane and detected with anti-HA mAb (lanes 1, 2, and 3) or anti-SARS-CoV S polyclonal antibody (lanes 4, 5, and 6). The molecular masses of marker proteins in kDa are shown on the left and the position of SARS-CoV S protein is indicated by an arrow on the right.

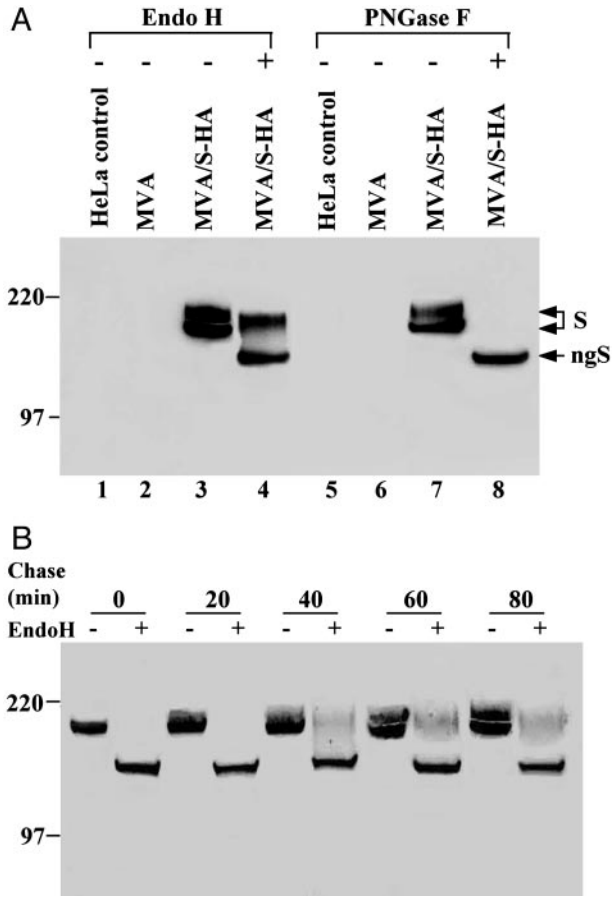

Fig. 2. Characterization of SARS-CoV S glycoprotein. (*A*) Endo H and PNGase F sensitivity. HeLa cells were uninfected (lanes 1 and 5), or infected with MVA (lanes 2 and 6) or MVA/S-HA (lanes 3, 4, 7, and 8). After 18 h, the cells were lysed, cleared by centrifugation, and incubated with anti-HA affinity matrix. The bound proteins were treated with endo H or PNGase F, as indicated by plus signs and were analyzed by SDS/PAGE and Western blotting with anti-HA mAb. The positions of two glycosylated forms of S and a nonglycosylated (ngS) form are shown by arrows. (*B*) Kinetics of endo H sensitivity. HeLa cells at 8 h after infection with MVA/S-HA were pulse-labeled with [^{35}S]methionine and [^{35}S]cysteine for 10 min and were then washed and chased for 0, 20, 40, 60, and 80 min in medium supplemented with unlabeled cysteine and methionine. Cells were lysed immediately after the pulse or chase and the S was captured with anti-HA affinity matrix, subjected to endo H digestion, resolved by SDS/PAGE, and visualized by autoradiography. The molecular masses of marker proteins in kDa are shown on the left.

The SARS-CoV S has 23 potential N-linked glycosylation sites (5), the use of which could contribute to the mass of the protein determined by SDS/PAGE. To evaluate this possibility, S expressed in HeLa cells was treated with PNGase F, which hydrolyzes all types of N-glycan chains. PNGase F treatment converted the 200-kDa doublet to a single sharp band of ≈160 kDa (Fig. 2*A*), which was still greater than the 135 kDa estimated from the gene sequence. However, differences of this magnitude between the theoretical mass and the mass estimated by SDS/PAGE are commonly found, and this discrepancy does not necessarily indicate that S contains additional posttranslational modifications.

Further experiments were carried out by using endo H, which digests the N-linked high-mannose carbohydrate side chains of glycoproteins that are synthesized in the endoplasmic reticulum, but not after conversion to a more complex form in the medial Golgi apparatus. Only a subpopulation of S was digested, because both the original size protein and a faster migrating one were detected (Fig. 2*A*). The latter had a slightly higher mass than the PNGase F-treated protein, which is consistent with N-acetylglucosamine residues remaining after hydrolysis by endo H. To determine the kinetics of acquisition of endo H resistance, cells infected with MVA/S-HA were pulse-labeled for 10 min with [^{35}S]methionine and [^{35}S]cysteine and were then chased in medium containing unlabeled amino acids. At each time point, the epitope-tagged S protein was isolated by using an HA mAb affinity matrix; one portion was analyzed directly by SDS/PAGE and autoradiography and an equal portion was first digested with endo H. Immediately after the pulse, we detected a sharp 200-kDa band that became more diffuse during the chase and was resolved as a doublet by 60 min in the absence of endo H treatment (Fig. 2*B*). The pulse-labeled S was completely digested to a 160-kDa species by endo H (Fig. 2*B*). A faint endo H-resistant band appeared by 40 min of chase (seen as a diffuse band in this particular experiment), indicating that a small fraction of S had become resistant to digestion (Fig. 2*B*). Even after 80 min, however, there was still considerable endo H-sensitive S.

Cellular Localization of S. The glycosylation and partial resistance to endo H was consistent with trafficking of the SARS-CoV S through the endoplasmic reticulum to the Golgi compartment. To determine whether S was expressed at the cell surface, unpermeabilized CEFs that had been infected with MVA/S were stained with antibody to S followed by Alexa 594-conjugated-anti-mouse IgG. Whereas the fluorescence due to coexpressed GFP was present throughout the cytoplasm, the labeling of S was restricted to the cell surface (Fig. 3*D*). Moreover, no labeling occurred in cells infected with the MVA vector (Fig. 3*B*) or uninfected cells (data not shown). Experiments were also carried out with cells infected with MVA/S-HA except that antibody to the epitope tag was used. The absence of staining of unpermeabilized cells (Fig. 3*F*) was consistent with the S protein having a type 1 topology with the tagged C terminus in the cytoplasm. After permeabilization of the plasma membrane with digitonin, both plasma membrane and juxtanuclear staining were evident (Fig. 3*H*). Similar patterns were found when infected HeLa cells were examined by confocal microscopy (data not shown).

Immunogenicity of MVA/S in Mice. Mice were inoculated i.n. or i.m. with 10^7 pfu of MVA/S at time 0 and again at 4 weeks. Antibody was determined by an endpoint ELISA using a recombinant protein consisting of the S1 domain of SARS-CoV made in insect cells and purified by affinity chromatography. Antibody was detected at 4 weeks and peaked at 6 weeks (Fig. 4*A*). Similar titers were obtained after either route of inoculation. The titers began to decline with time and were not boosted at 2 weeks after the SARS-CoV challenge described in the next section (Fig. 4*A*).

The ability of sera to neutralize SARS CoV infectivity for VERO cells was determined as described (14). Neutralizing antibody was detected after the second immunization by either the i.n. or i.m. route (Fig. 4*B*).

Protection of Mice Immunized with MVA/S. Previous studies (14) demonstrated that mice inoculated i.n. with SARS-CoV exhibit no overt signs of disease, but have elevated virus titers in the respiratory tract that peak within 2 days and are cleared by 7 days. For the present study, we had three control and two experimental groups. The controls were mice that were uninoculated or that had received the MVA vector i.m. or i.n.. When these mice were challenged with 10^4 $TCID_{50}$ of SARS-CoV, $\approx 10^5$ TCID50 of SARS-CoV per g of lung was recovered on day 2 (Fig. 5). By contrast, the titers of SARS-CoV from the lungs of mice immunized with MVA/S either i.m. or i.n. were reduced to levels that were barely above the limit of detection (Fig. 5). Approximately 10^3 $TCID_{50}$ per g of SARS-CoV were recovered from the nasal turbinates of control mice, but this amount too was significantly reduced in the immunized animals (Fig. 5). The severe reduction in SARS-CoV replication may explain the absence of an amnestic ELISA antibody response to S after challenge (Fig. 4*A*). Neutralizing titers to SARS CoV were not measured after challenge.

Passive Protection Mediated by Serum from MVA/S-Immunized Mice. MVA can induce both humoral and cell mediated immune responses. To determine a role for antibody, we pooled sera from mice that had been immunized i.m. with 10^7 pfu of MVA/S or MVA on day 0 and 28 and were bled 3 weeks later. The reciprocal ELISA titer to S1 was $\approx$1:25,000 and the mean neutralizing titer was 1:284. Undiluted or diluted serum (0.4 ml) was administered i.p. to naïve mice to evaluate the protective role of antibody. As a positive control, we administered hyperimmune SARS-CoV serum to two mice (14). On the next day, the mice received an i.n. challenge of 10^5 $TCID_{50}$ of SARS-CoV, and 2 days later, their nasal turbinates and lungs were removed to measure the virus titers. Administration of undiluted MVA/S serum reduced the lung titers by $10^{5.1}$ (Table 1), compared with recipients of MVA control serum, indicating that antibodies to the SARS CoV S conferred the observed protection. Protection was observed despite only achieving a neutralization titer of 1:35 in recipient mice. Replication of SARS-CoV increased as the quantity of passively transferred serum decreased, but significant reductions in lung virus titers still occurred at dilutions of 1:4, 1:16, and 1:64. The absence of detectable neutralizing antibody in mice receiving these dilutions of passively transferred serum probably reflects a low sensitivity of the *in vitro* neutralization assay,

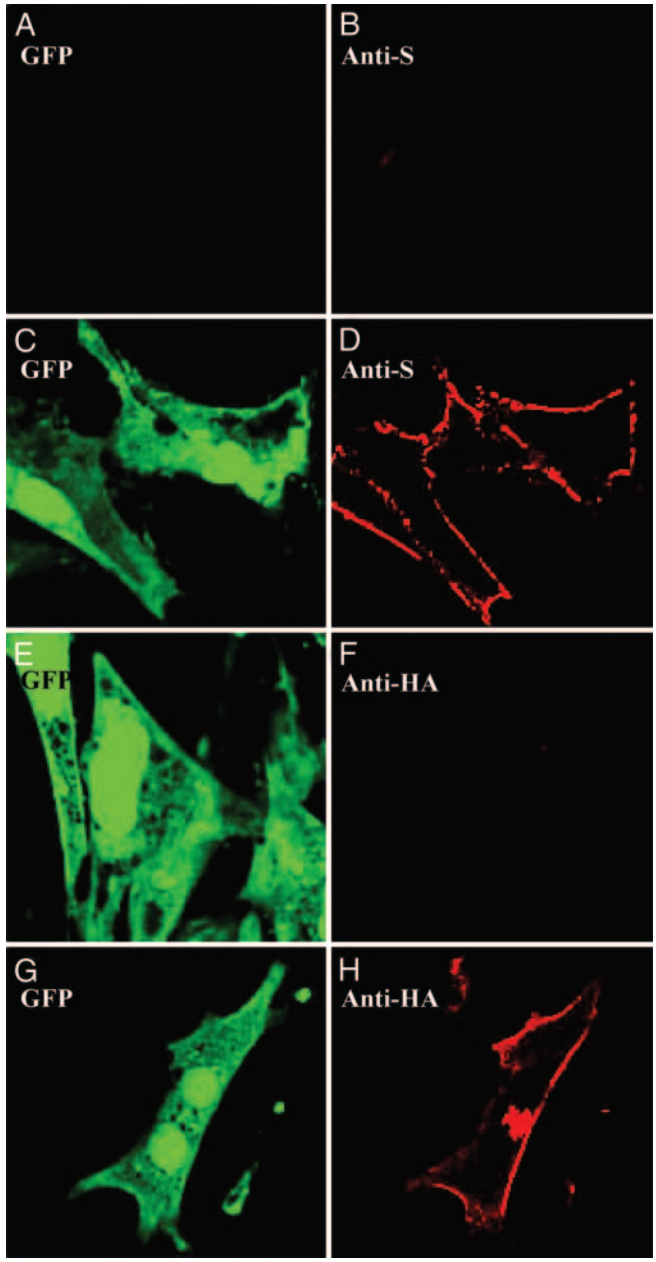

Fig. 3. Cellular localization of SARS-CoV S. Unfixed and unpermeabilized CEF (*A–F*) that had been infected with MVA (*A* and *B*), MVA/S (*C* and *D*), and MVA/S-HA (*E* and *F*) for 18 h were stained with anti-SARS-CoV mouse serum (*A–D*) or anti-HA mAb (*E* and *F*), followed by Alexa 594-conjugated anti-mouse IgG and viewed by confocal microscopy. CEF infected with MVA/S-HA (*G* and *H*) were fixed, permeabilized, and stained with anti-HA mAb, followed by Alexa 594-conjugated anti-mouse IgG. Shown are GFP (*Left*) and Alexa 594 (*Right*) fluorescence, respectively.

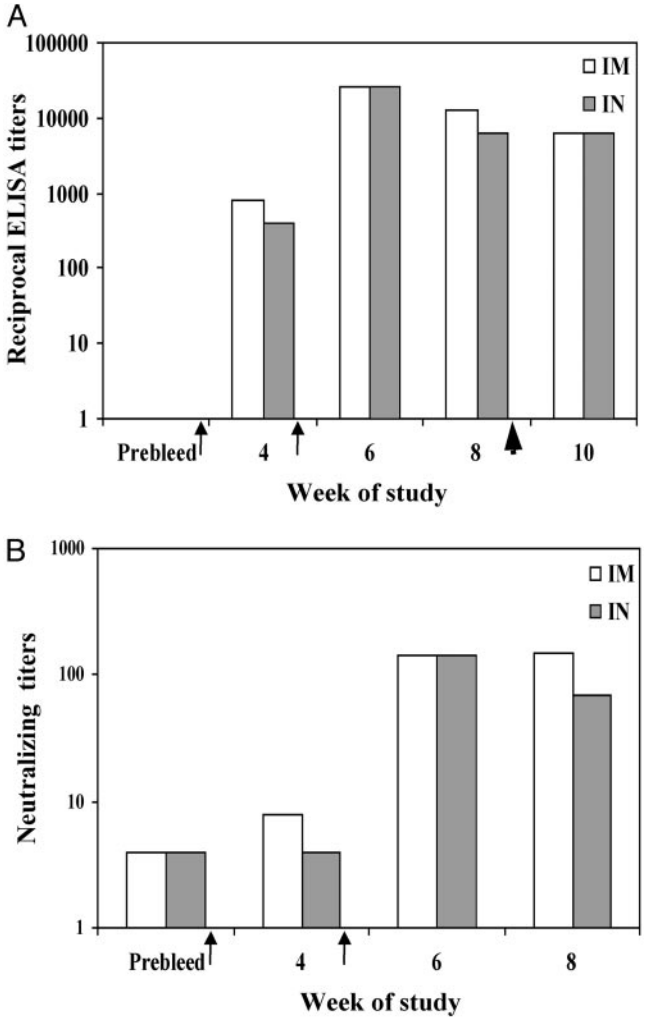

Fig. 4. Antibody responses after immunization with recombinant MVA/S by an i.n. or i.m. route. (*A*) End point ELISA titers of pooled serum ($n = 8$), taken before (pre-bleed) or after immunizations, were determined by using insect cell-expressed S1 domain of the SARS-CoV S as the capture antigen. Sera from two mice were pooled after challenge and analyzed. Thin and thick arrows depict times of immunizations and challenge with SARS-CoV, respectively. (*B*) Prechallenge SARS-CoV neutralization titers of pooled serum were determined. The dilution of serum that completely prevented SARS-CoV cytopathic effect in 50% of the wells was calculated.

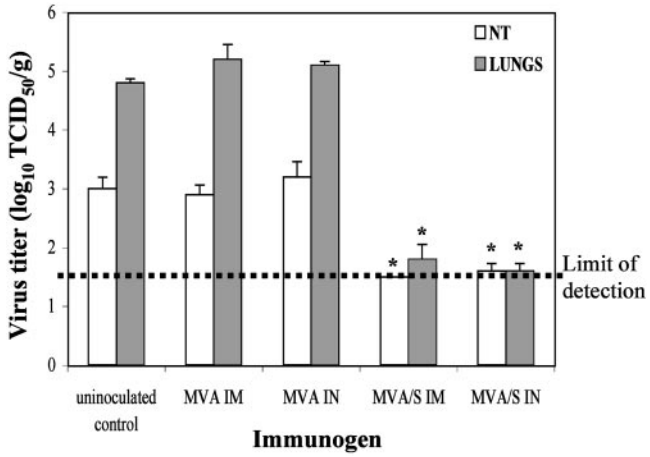

Fig. 5. Protection of immunized mice from subsequent challenge with SARS-CoV. Groups of eight BALB/c mice were mock-vaccinated or vaccinated with MVA or MVA/S by the i.n. or i.m. route at time 0 and 4 weeks, and were challenged 4 weeks later with 10^4 $TCID_{50}$ of SARS-CoV administered by the i.n. route. Two days later, the titers of SARS-CoV in the lungs and nasal turbinates of four mice in each group were determined. Virus titers are expressed as $\log_{10}$ $TCID_{50}$ per g of tissue. Statistical comparison of MVA/S titers to unvaccinated controls was performed by using a Mann–Whitney *U* nonparametric analysis; *, $P = 0.02$.

because the ELISA titers to S were >100-fold higher than the neutralization titers (Fig. 4). The recovery of SARS-CoV from the nasal turbinates was also reduced, but to a relatively lesser extent than from the lungs.

Discussion

Our object was to express S in a native state to induce antibodies that would neutralize SARS-CoV. The secretory pathway of the cell has an important quality control function, and the trafficking of a protein from the endoplasmic reticulum to the plasma membrane is a sign of proper folding. The N-linked oligosaccharide pathway is frequently used for tracking protein movement. Addition of N-linked oligosaccharides occurs in the endoplasmic reticulum and the conversion of the high mannose form to complex endo H-resistant N-linked chains occurs on transport from the cis to the medial Golgi compartment. We found that the S ORF of SARS-CoV was expressed by recombinant MVA as a protein of ≈200 kDa, which was reduced to 160 kDa by a glycosidase specific for N-linked carbohydrates. Trafficking of S to the medial Golgi apparatus was indicated by acquisition of endo H resistance by a subpopulation of molecules within 40 min after pulse labeling. The staining of the surface of unpermeabilized cells infected with MVA/S by S-specific antibody provided direct evidence for insertion into the plasma membrane. Furthermore, the inability of antibody to a C-terminal epitope tag to stain cells unless they were permeabilized indicated that S has a type 1 topology in the membrane. We did not detect putative S1 and S2 cleavage products, as found for group 2 but not group 1 CoV S proteins (28). Xiao *et al.* (13) expressed full-length S by transfection and detected low amounts of several smaller than full-length S fragments, which they suggested might include specific cleavage products, although no evidence to support this hypothesis was presented. Our characterization studies strongly suggested that MVA expressed a properly folded form of S, leading us to determine whether it would elicit neutralizing antibodies.

Mice immunized with MVA/S by i.n. or i.m. routes developed antibodies that bound to the S1 domain of S and neutralized SARS-CoV *in vitro*. Furthermore, mice immunized i.m. or i.n. exhibited little or no replication of SARS CoV in the upper and lower respiratory tracts after an i.n. inoculation. Control mice vaccinated with the MVA vector by i.n. or i.m. routes were unprotected, indicating that the effect was specific for the expressed S protein and was not due to enhanced nonspecific immunity. The ability of i.m. or i.n. inoculation of a recombinant MVA to prevent upper and lower respiratory infections had previously been found in a rodent model of parainfluenza virus 3 (25).

Previous studies (14) showed that i.p. inoculation of hyperimmune serum from mice inoculated twice with SARS CoV provided protection against SARS-CoV in the lower respiratory tract and to a lesser extent in the upper respiratory tract (14). Protection with serum from MVA/S-immunized animals was demonstrated in the present study. Because serum from animals inoculated with the MVA vector had no effect, we can attribute the protection to S-specific antibodies. These results indicated that the S of SARS CoV, like that of other CoV, is an important target of neutralizing antibody both *in vitro* and *in vivo*. Recently, mAbs specific to SARS-CoV S1 domain with *in vitro* neutralizing

Table 1. Inhibition of virus replication in respiratory tract after passive transfer of serum from immunized mice

			Virus replication in challenged mice†					
			Nasal turbinates			Lungs		
Passively transferred Ab*	Neutralizing titer of Ab given	Geometric mean neutralizing titer in recipient mice	Mean ± SE virus titer‡	No. infected/ no. tested	*P*§	Mean ± SE virus titer‡	No. infected/ no. tested	*P*§
MVA/S undiluted	1:284	1:35	2.9 ± 0.57	2/3	0.08¶	1.7 ± 0.17	1/3	0.03
MVA/S 1:4	1:71	<1:8	2.4 ± 0.32	2/4	0.02	3.2 ± 0.58	3/4	0.02
MVA/S 1:16	1:18	<1:8	2.5 ± 0.39	2/4	0.02	5.5 ± 0.20	4/4	0.03
MVA/S 1:64	<1:16	<1:8	3.4 ± 0.58	4/4	0.19	6.0 ± 0.10	4/4	0.02
MVA/S 1:128	<1:16	<1:8	3.4 ± 0.36	4/4	0.11	6.5 ± 0.25	4/4	0.25
MVA undiluted	<1:16	<1:8	4.0 ± 0.20	4/4	–	6.8 ± 0.25	4/4	–
SARS-CoV 1:4	1:512	1:17	≤1.8 ± 0‖	0/2	0.06¶	≤1.5 ± 0‖	0/2	0.06¶

*The indicated dilutions of antibody in 400 μl were administered to recipient mice by i.p. injection.
†Mice were challenged with 10^5 $TCID_{50}$ SARS-CoV i.n.
‡Virus titers are expressed as $\log_{10}$ $TCID_{50}$ per g of tissue
§*P* values comparing titers with those seen in mice that received undiluted MVA control antibody in a Mann–Whitney *U* nonparametric analysis.
¶Small sample size affected statistical significance.
‖Virus not detected; the lower limit of detection of infectious virus in a 5% wt/vol suspension of nasal turbinates was 1.8 $\log_{10}$ $TCID_{50}$ per g and in a 10% wt/vol suspension of lung homogenate was 1.5 $\log_{10}$ $TCID_{50}$ per g.

activity were described (29), and it will be interesting to test them *in vivo*.

No enhanced virus replication or obvious disease was found in mice that were immunized with MVA/S before challenge with SARS-CoV, as has been found after immunization with a vaccinia virus vector expressing S from feline infectious peritonitis virus and challenge with the corresponding virus (30). The latter effect is thought to be due to S antibody-dependent enhanced infection of macrophages (31, 32). Although it will be necessary to look for enhanced antibody effects in other animal models of SARS-CoV, the present study is encouraging for the development of SARS-CoV vaccines based on the highly attenuated MVA vector expressing S.

We thank Linda Wyatt for assistance in isolating recombinant MVA and Larry Anderson for a sample of SARS-CoV mouse serum and for critical reading of the manuscript.

1. Drosten, C., Gunther, S., Preiser, W., van der Werf, S., Brodt, H. R., Becker, S., Rabenau, H., Panning, M., Kolesnikova, L., Fouchier, R. A. *et al.* (2003) *N. Engl. J. Med.* **348,** 1967–1976.
2. Ksiazek, T. G., Erdman, D., Goldsmith, C. S., Zaki, S. R., Peret, T., Emery, S., Tong, S., Urbani, C., Comer, J. A., Lim, W., *et al.* (2003) *N. Engl. J. Med.* **348,** 1953–1966.
3. Peiris, J. S., Lai, S. T., Poon, L. L., Guan, Y., Yam, L. Y., Lim, W., Nicholls, J., Yee, W. K., Yan, W. W., Cheung, M. T., *et al.* (2003) *Lancet* **361,** 1319–1325.
4. Kuiken, T., Fouchier, R. A., Schutten, M., Rimmelzwaan, G. F., van Amerongen, G., van Riel, D., Laman, J. D., de Jong, T., van Doornum, G., Lim, W., *et al.* (2003) *Lancet* **362,** 263–270.
5. Rota, P. A., Oberste, M. S., Monroe, S. S., Nix, W. A., Campagnoli, R., Icenogle, J. P., Penaranda, S., Bankamp, B., Maher, K., Chen, M. H., *et al.* (2003) *Science* **300,** 1394–1399.
6. Marra, M. A., Jones, S. J., Astell, C. R., Holt, R. A., Brooks-Wilson, A., Butterfield, Y. S., Khattra, J., Asano, J. K., Barber, S. A., Chan, S. Y., *et al.* (2003) *Science* **300,** 1399–1404.
7. Guan, Y., Zheng, B. J., He, Y. Q., Liu, X. L., Zhuang, Z. X., Cheung, C. L., Luo, S. W., Li, P. H., Zhang, L. J., Guan, Y. J., *et al.* (2003) *Science* **302,** 276–278.
8. Holmes, K. V. (2003) *J. Clin. Invest.* **111,** 1605–1609.
9. Lai, M. M. & Cavanagh, D. (1997) *Adv. Virus Res.* **48,** 1–100.
10. Lai, M. M. C. & Holmes, K. V. (2001) in *Fundamental Virology*, eds. Knipe, D. M. & Howley, P. M. (Lippincott, Williams & Wilkins, Philadelphia), pp. 641–664.
11. Navas-Martin, S. & Weiss, S. R. (2003) *Viral Immunol.* **16,** 461–474.
12. Li, W., Moore, M. J., Vasilieva, N., Sui, J., Wong, S. K., Berne, M. A., Somasundaran, M., Sullivan, J. L., Luzuriaga, K., Greenough, T. C., *et al.* (2003) *Nature* **426,** 450–454.
13. Xiao, X., Chakraborti, S., Dimitrov, A. S., Gramatikoff, K. & Dimitrov, D. S. (2003) *Biochem. Biophys. Res. Commun.* **312,** 1159–1164.
14. Subbarao, K., McAuliffe, J., Vogel, L. K., Fahle, G., Fischer, S., Tatti, K., Packard, M., Shieh, W.-J., Saki, S. & Murphy, B. (2004) *J. Virol.* **78,** 3572–3577.
15. Moss, B. (1996) *Proc. Natl. Acad. Sci. USA* **93,** 11341–11348.
16. Mayr, A. (1967) *Zentralbl. Bakteriol. Mikrobiol. Hyg. Abt. 1 Orig. B*, 183–189.
17. Meyer, H., Sutter, G. & Mayr, A. (1991) *J. Gen. Virol.* **72,** 1031–1038.
18. Antoine, G., Scheiflinger, F., Dorner, F. & Falkner, F. G. (1998) *Virology* **244,** 365–396.
19. Carroll, M. & Moss, B. (1997) *Virology* **238,** 198–211.
20. Drexler, I., Heller, K., Wahren, B., Erfle, V. & Sutter, G. (1998) *J. Gen. Virol.* **79,** 347–352.
21. Blanchard, T. J., Alcami, A., Andrea, P. & Smith, G. L. (1998) *J. Gen. Virol.* **79,** 1159–1167.
22. Sutter, G. & Moss, B. (1992) *Proc. Natl. Acad. Sci. USA* **89,** 10847–10851.
23. Stittelaar, K. J., Kuiken, T., de Swart, R. L., van Amerongen, G., Vos, H. W., Niesters, H. G., van Schalkwijk, P., van der Kwast, T., Wyatt, L. S., Moss, B. & Osterhaus, A. D. (2001) *Vaccine* **19,** 3700–3709.
24. Wyatt, L. S., Earl, P. L., Eller, L. A. & Moss, B. (2004) *Proc. Nat. Acad. Sci. USA* **101,** 4590–4595.
25. Wyatt, L. S., Shors, S. T., Murphy, B. R. & Moss, B. (1996) *Vaccine* **14,** 1451–1458.
26. Earl, P. L., Moss, B., Wyatt, L. S. & Carroll, M. W. (1998) in *Current Protocols in Molecular Biology*, eds. Ausubel, F. M., Brent, R., Kingston, R. E., Moore, D. D., Seidman, J. G., Smith, J. A. & Struhl, K. (Greene Publishing Associates & Wiley Interscience, New York), Vol. 2, pp. 16.17.1–16.17.19.
27. Reed, L. J. & Muench, H. (1938) *Am. J. Hyg.* **27,** 493–497.
28. Gallagher, T. M. & Buchmeier, M. J. (2001) *Virology* **279,** 371–374.
29. Sui, J., Li, W., Murakami, A., Tamin, A., Matthews, L. J., Wong, S. K., Moore, M. J., Tallarico, A. S., Olurinde, M., Choe, H., *et al.* (2004) *Proc. Natl. Acad. Sci. USA* **101,** 2536–2541.
30. Vennema, H., de Groot, R. J., Harbour, D. A., Dalderup, M., Gruffydd-Jones, T., Horzinek, M. C. & Spaan, W. J. (1990) *J. Virol.* **64,** 1407–1409.
31. Corapi, W. V., Olsen, C. W. & Scott, F. W. (1992) *J. Virol.* **66,** 6695–6705.
32. Olsen, C. W., Corapi, W. V., Ngichabe, C. K., Baines, J. D. & Scott, F. W. (1992) *J. Virol.* **66,** 956–965.